AJNR Am J Neuroradiol 23:716–723, April 2002

Value of MR Imaging of the Brain in Children with Hypoxic Coma

Catherine Christophe, Christine Fonteyne, France Ziereisen, Florence Christiaens, Paul Deltenre, Viviane De Maertelaer, and Bernard Dan

BACKGROUND AND PURPOSE: **The contribution of MR imaging to identify hypoxic-ischemic injuries has been studied mostly in neonates or adults. The purpose of this study was to describe the MR imaging findings of toddlers and older children with hypoxic coma and to analyze the prognostic value of an MR imaging scoring system.**

METHODS: **The conditions of 40 children with hypoxic coma (age range, 6 weeks to 18 years) were clinically graded according to the pediatric risk of mortality score, and MR imaging studies were performed. Sixty-four MR imaging studies were distributed in five categories according to their timing relative to the hypoxic event: days 1 through 3, 4–7, 8–15, 16–50, and after day 50. These were evaluated retrospectively by using an eight-point scoring system based on two lesion categories assessing watershed areas and basal ganglia involvement, including signal intensity and morphologic features with respect to maturation-related norms. Two age groups (≤1 year and >1 year) were considered. The surviving children were grouped according to neurologic outcome.**

RESULTS: **The occurrence of watershed areas or basal ganglia involvement was not significantly different in association with age. Sixteen children died. Twelve children had moderate to severe sequelae resulting from neurodevelopmental disabilities, and 12 had good neurologic outcomes. There was no correlation between pediatric risk of mortality score and neurologic evolution. There was a strong correlation between first MR imaging score ($P < .001$) and neurologic outcome. The sensitivity of the first MR imaging score was high (96%), even when obtained during the first 3 days, with a specificity of 50% and a positive predictive value of 82%. Six patients with definite abnormal MR imaging findings experienced good neurologic outcomes.**

CONCLUSION: **The MR imaging scoring system proposed in this study can be used to establish an early prognosis in a significant proportion of children with hypoxic coma. It is helpful, even during the first 3 days after the event. However, some patients with definite abnormal MR imaging findings may experience good neurologic evolution.**

With improved specialized management resources, an increasing proportion of post-hypoxic comatose children survive. In this context, it may be difficult to identify children who will have good outcomes and those who will die or have a poor neurologic prognosis associated with hypoxic-ischemic encephalopathy. Reliable neurologic evaluation of comatose children in intensive care is often difficult because of medication and metabolic changes. A survey of the literature reveals that neurologic and neurophysiologic findings of patients older than 10 years with anoxic-ischemic coma could identify a subgroup of irrecoverable patients only after 72 hours of coma (1, 2). On the other hand, neurodiagnostic imaging has proved to be helpful in depicting hypoxic-ischemic cerebral injuries, as these findings may allow prediction of neurodevelopmental outcome. MR imaging is now recognized as the primary diagnostic tool in the evaluation of infarction. However, the neuropathologic pattern of hypoxic-ischemic encephalopathy varies not only with the severity and duration of the hypoxia but also with the state of brain maturation. Until recently, the contribution of MR imaging has been studied mostly in premature and full-term neonates (3–12) and in adults (13–16). Few studies were focused on toddlers and older children (17, 18). The aim of this study was to illustrate the MR imaging patterns of cerebral lesions associated with coma due to hypoxic-ischemic

Received March 20, 2001; accepted after revision October 22.

From the Departments of Imaging (C.C., F.Z.) and Pediatrics (C.F., F.C., B.D.), Hôpital Universitaire des Enfants Reine Fabiola; the Department of Neurology (P.D.), Centre Hospitalier Universitaire Brugmann; and IRIBHN (V.D.M.), Statistical Unit, Free University of Brussels, Belgium.

Address reprint requests to Catherine Christophe, Hôpital Universitaire des Enfants Reine Fabiola, 15 av. J. J. Crocq, B-1020 Brussels, Belgium.

encephalopathy in children from infancy to adolescence and to evaluate the prognostic value of MR imaging for the neurodevelopmental and vital outcomes.

Methods

Study Population

The study group consisted of 40 consecutive children (18 girls and 22 boys; age range, 6 weeks to 18 years; mean age, 2.6 years) who were admitted to the pediatric intensive care unit of a children's hospital during a 7-year period for hypoxic coma and who had undergone MR imaging. The criterion for hypoxic coma was coma with a partial pressure of oxygen in arterial blood reading of <60 mmHg. Neonates and children with metabolic or traumatic coma were excluded. The medical records of these 40 children were retrospectively reviewed. The cause of hypoxia was ischemic in 11 patients (septic shock in seven and hypovolemic shock in four) and anoxic-hypoxic in 29 (complication of anesthesia or sedation in three, near-drowning in four, airway obstruction or respiratory insufficiency in five, methadone intoxication in one, hypoxia associated with hypoglycemia in one, and hypoxia of unknown origin in 15). Fifteen (38%) children had experienced cardiac arrest for more than 5 min, 30 (75%) had experienced seizures during the acute phase, and 38 (95%) required intubation.

The conditions of the 40 children were graded according to the pediatric risk of mortality (PRISM) score (19) during the first 24 hr after admission to the pediatric intensive care unit. The PRISM score consists of 14 routinely measured physiological variables, including hemodynamic (systolic blood pressure, diastolic blood pressure, heart rate), respiratory (respiratory rate, partial pressure of oxygen in arterial blood/fractional inspired oxygen, arterial carbon dioxide pressure), neurologic (modified Glasgow Coma Scale score, pupillary reactions), metabolic (bilirubin, potassium, calcium, glucose, bicarbonate), and coagulation (Quick's, or prothrombin test) parameters. The theoretic maximal score is 76, indicating the highest mortality risk. The median PRISM score was 27 (range, 7–47). The median modified Glasgow Coma Scale score was 3 (range, 3–12).

Imaging Techniques and Evaluation

MR examinations were performed at 0.5 T. For all patients, the basic examination protocol included a T1-weighted spin-echo sequence in the sagittal and axial planes (500/35 [TR/TE]) and then a combined proton density– and T2-weighted spin-echo sequence (3700/35, 150 [TR/first TE, second TE]) in the axial plane. A T1-weighted phase-sensitive inversion recovery sequence (1600/600/35, TR/TE/TI) was also obtained in the axial plane for children younger than 2 years and a fluid-attenuated inversion recovery sequence (FLAIR) (6000/2000/150) was obtained in the coronal plane, when available, for children older than 2 years. Contrast injection with gadolinium-diethylenetriamine pentaacetic acid at a dose of 0.1 mmol/kg was obtained in 20 MR imaging examinations based on practical (timing, personnel availability, etc) rather than clinical considerations. Children requiring assisted ventilation received manually administered ventilation while in the magnet. All children were monitored with ECG and pulse oximeter. If anesthesia was necessary, propofol (Diprivan) was administered IV. Of these 40 children, 21 underwent MR imaging once; 14, twice; and five, three times.

The 64 MR imaging studies were distributed in five classes according to time since onset of coma: hyperacute (class A), performed on days 1–3; acute (class B), performed on days 4–7; early subacute (class C), performed on days 8–15; late subacute (class D), performed on days 16–50; and chronic (class E), performed after day 50. The 64 MR imaging studies were evaluated retrospectively by using a scoring system based on two basic lesion categories assessing watershed areas and basal ganglia involvement (Table 1). Cerebral cortex, deep gray matter nuclei, and deep and subcortical white matter were analyzed. Changes in signal intensity and morphologic features were recorded with respect to the normal MR imaging brain pattern according to norms of brain maturation. Morphologic criteria included parenchymal swelling or distortion of normal adjacent structures (obliteration of sulci and cisterns, ventricular compression, tonsillar protrusion, loss of normal flow voids in circle of Willis circulation, etc). The images were assessed independently by two experienced pediatric neuroradiologists (C.C., F.Z.). One radiologist was unaware of the patients' histories.

TABLE 1: MR imaging scoring system

Watershed area involvement	
Absent	0
Possible signs of infarction (mild swelling or mild signal changes)	1
Definite signs of infarct	
In the anterior or posterior boundary zones	2
In the anterior and posterior boundary zones or diffuse unilateral	3
Diffuse bilateral	4
Basal ganglia involvement	
Absent	0
Possible signs of infarction (fuzzy margins, swelling, mild diffuse signal changes or peripheral signal changes)	1
Definite signal changes	
One of the basal ganglion	2
Two of the basal ganglia	3
Three or more basal ganglia (globus pallidus and putamen were considered together as lentiform nuclei)	4
Theoretic maximum	8
(Score of 8 was also attributed for signs of cerebral herniation)	

The total theoretic maximum for the MR imaging scoring system was 8, as for severe signs of diffuse edema with cerebral herniation. A definite abnormal MR imaging finding was defined by a score >2 and normal or subnormal by a score ≤2. As in the literature, there were differences between MR imaging findings of infants (3–12) and older patients (13–18), we therefore considered two age groups: 20 children aged 6 weeks to 1 year (group 1) and 20 children older than 1 year to 18 years (group 2).

Clinical Outcome

The surviving children were reviewed by a pediatric neurologist who performed neurodevelopmental testing, assessing the neurologic evolution from 1 month to 8 years (mean, 30 months) after presentation. The neurologic evolution was scored in terms of motor function (no impairment = 0, mild = 1, moderate = 2, and severe = 3), cognitive function (no impairment = 0, mild = 1, moderate = 2, and severe = 3), and seizure disorder (no seizures = 0, seizures easily controlled with medical treatment = 1, seizures controlled with difficulty = 2, and seizures uncontrolled with medication = 3). The total theoretic maximum for the neurologic evolution score was 9. For each patient, only the best ever achieved neurologic evolution score was used. A score of 10 was assigned to the deceased children. A good neurologic evolution corresponded to a score of ≤2. A bad neurologic evolution corresponded to a score of >2, which indicated a change ranging from moderate to severe (neurologic evolution score >2 and <8) to persistent vegetative state (neurologic evolution ≥8) or death (neurologic evolution = 10).

Statistical Analysis

Interobserver agreement regarding the MR imaging score was assessed by the weighted kappa coefficient, which was tested by using the Monte Carlo procedure (20): $\kappa > 0.81$, agreement very good; $\kappa = 0.61–0.8$, good agreement; $\kappa = 0.41–0.6$, moderate agreement; $\kappa = 0.21–0.4$, fair agreement;

TABLE 2: MR imaging findings (n = 64)

		Watershed Area Involvement						Basal Ganglia Involvement				
Group	Normal	Cortical Swelling	Cortical and White Matter or Cortical and Subcirtical T2/PD*†	Cortical T1†	Cortical T2‡	Clear Atrophy	Doubtful or Pseudoatrophy	Fuzzy	T2†	T2‡	T1†	T2‡
1§	1 (B)	12 (A–C)	31 (A–E)	13 (B–D)	20 (A–D)	7 (C, D)	5 (C, D)	10 (A–E)	18 (A–E)	10 (A–D)	4 (A–C)	4 (C, D)
2‖	2 (B, C)	9 (A–D)	26 (A–E)	NA	2 (B, C)	6 (D, E)	10 (B–D)	16 (A–D)	22 (A–E)	NA	1 (C)	3 (C, D)

Note.—A indicates lesion observed on days 1–3; B, lesion observed on days 4–7; C, lesion observed on days 8–15; D, lesion observed on days 16–50; E, lesion observed after day 50; NA, not applicable; T1, T1-weighted imaging; T2, T2-weighted imaging; PD proton density–weighted imaging.

*Cortical and white matter for group 1, cortical and subcortical for group 2.

†Lesion was hyperintense compared with normal brain tissue.

‡Lesion was hypointense compared with normal brain tissue.

§Twenty patients, 33 MR imaging findings, <1 year.

‖ Twenty patients, 31 MR imaging findings, >1 year.

and $\kappa = 0-0.2$, poor agreement. Age, PRISM score, and first MR imaging score were correlated with neurologic evolution score. To study the impact of delay in obtaining MR images, all MR imaging scores were further analyzed based on five smaller time frames (classes A–E) according to delay in obtaining MR images after onset of coma.

Cardiac arrest lasting >5 minutes and basal ganglia involvements were correlated with neurologic evolution. Occurrence of watershed areas or basal ganglia involvement was correlated with the two age groups. Continuous data were compared among groups by using the Mann-Whitney test. The strength of the correlations between two variables was assessed with the Spearman correlation coefficient. Tests of the absence of correlations were performed. Associations between polytomous variables were assessed with the use of classical χ^2 tests when the required large sample conditions were satisfied. Otherwise, exact tests were applied. In this case, calculations were made with StatXact4 statistical software (Cytel, MA).

Results

MR Imaging Findings

The main MR imaging data are summarized in Tables 2–4. Table 2 shows the ranges of MR imaging findings of the 64 MR imaging studies according to timing of imaging (classes of MR images on which the lesion was observed) and according to age groups. One infant in group 1 and two children in group 2 had normal MR imaging findings.

Although MR imaging findings may vary with timing relative to the hypoxic event, many features could be observed through several classes (Table 2). On the first MR images, 13 infants in group 1 and 16 children in group 2 had definite signs of watershed areas in-

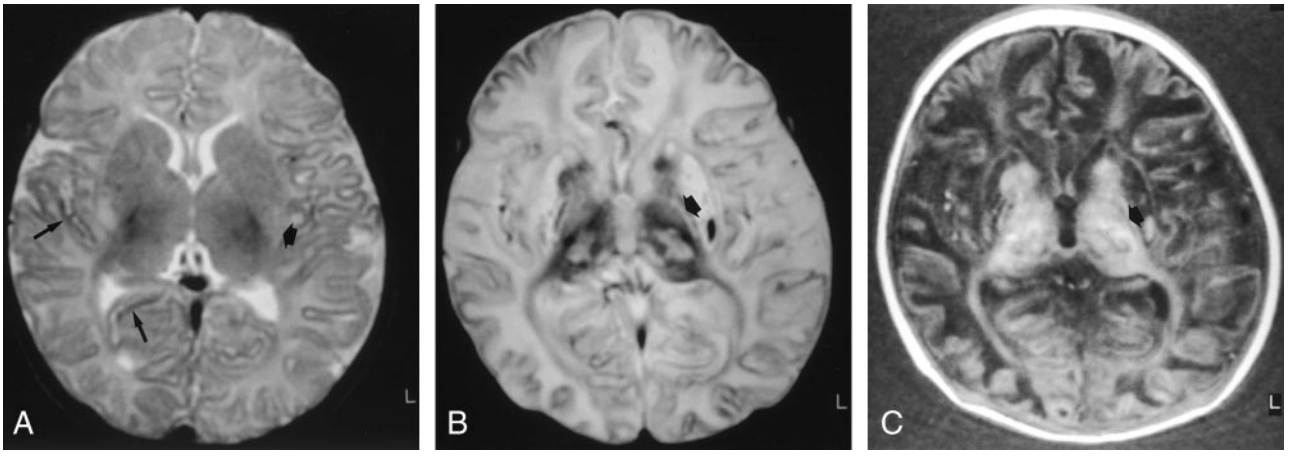

FIG 1. Images of a patient who experienced cardiorespiratory arrest of unknown cause at age 2.5 months. The infant died 18 days after the event.

A, Axial spin-echo T2-weighted image (3700/150), obtained 28 hours after the event (class A), shows mild cortical and white matter hyperintensity, consistent with edema, and mild focal cortical T2 hypointensity (*long arrows*). Watershed areas score, 1/4. Fuzzy hyperintense areas (*short arrow*) are also seen in the posterior lentiform nuclei. Basal ganglia score, 1/4; total MR imaging score, 2/8.

B, Axial spin-echo T2-weighted image (3700/150), obtained 16 days after the event (class C). Diffuse T2 hyperintensity and loss of gray-white matter differentiation are consistent with severe cortical and white matter involvements. Focal cortical T2 hypointensity was also seen. Watershed areas score, 4/4. Prominent involvements in all the basal ganglia are present in caudate nuclei, lentiform nuclei, and thalami as important signal intensity modifications (abnormal hyperintense and hypointense areas). Basal ganglia score, 4/4. There is, moreover, an involvement in the posterior limb of the internal capsule as T1 and T2 prolongation (*arrow*). Total MR imaging score, 8/8.

C, Axial inversion-recovery T1-weighted image (1600/600/35), obtained 16 days after the event (class C). T1 hyperintensity was also seen. Watershed areas score, 4/4. Prominent involvements in all the basal ganglia are present in caudate nuclei, lentiform nuclei, and thalami as important signal intensity modifications (abnormal hyperintense and hypointense areas). Basal ganglia score, 4/4. There is, moreover, an involvement in the posterior limb of the internal capsule as T1 and T2 prolongation (*arrow*). Total MR imaging score, 8/8.

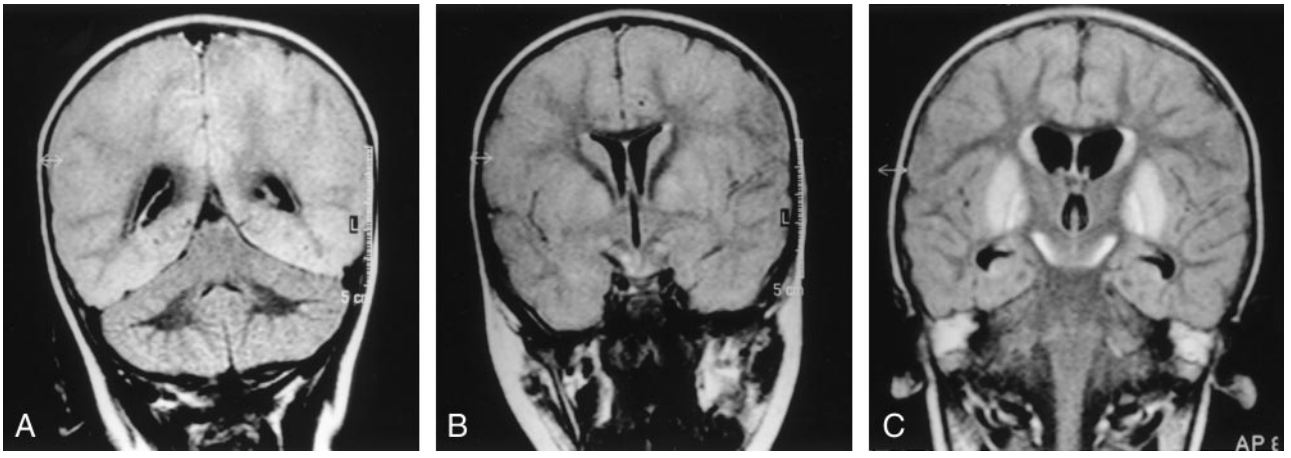

FIG 2. Images of a patient who experienced near-drowning at age 21-months. The patient died 16 days after the event.

A, Coronal T2-weighted FLAIR image (6000/2000/150), obtained 7 days after the event (class B), shows supratentorial moderate cortical tumefaction and hyperintensity (compared with the cerebellar cortex). Watershed areas score, 4/4.

B, Coronal T2-weighted FLAIR image (6000/2000/150), obtained 7 days after the event (class B). Basal ganglia involvement can be seen with fuzzy margins and T2 hyperintensity (lentiform nuclei, caudate nuclei, and subthalamic nuclei hyperintensity). Basal ganglia score, 4/4; total MR imaging score, 8/8.

C, Coronal T2-weighted FLAIR image (6000/2000/150), obtained 14 days after the event (class C). The cortex is no longer swollen but is still diffusely hyperintense. Watershed areas score, 4/4. More prominent basal ganglia hyperintensity can be seen. Basal ganglia score, 4/4; total MR imaging score, 8/8.

volvement (MR imaging watershed areas score >1). Nine infants in group 1 and 13 children in group 2 had definite signs of basal ganglia involvement (MR imaging basal ganglia score >1). The occurrence of watershed areas or basal ganglia involvement was not significantly different between age groups ($P = .288$ and $P = .341$, respectively). However, the pattern of signal changes was more varied in group 1 than in group 2.

Watershed areas involvement in group 1 appeared as cortical swelling best identified on the T1-weighted images or as signal modifications: cortical and white matter hyperintensity on T2-weighted (Fig 1B) and proton density–weighted images, cortical hyperintensity on T1-weighted images (Fig 1C), or focal cortical hypointensity on T2-weighted images (Fig 1B). White matter lesions were more common in group 1 than in group 2.

Watershed areas involvement in group 2 appeared essentially as cortical swelling (Fig 2A and B and Fig 3), cortical hyperintensity on T2-weighted images (Fig 2A and B, Fig 3), or stripe of hyperintensity in the cortex and at the cortex-white matter junction on T2- or proton density–weighted sequences (as tram tracks) (Fig 3A). Less often, focal T2 shortening of the cortex could be seen.

The MR imaging anomalies tended to predominate in arterial border zones in the parasagittal regions, in end zones in the depths of sulci in both groups, and in the highly myelinating perirolandic region in group 1. In both groups, watershed areas involvement tended to evolve with time from cortical swelling with T1-, proton density–, and T2-weighted signal changes to cortical atrophy and T2 prolongation.

Basal ganglia involvement in group 1 appeared as fuzzy basal ganglia margins, T2 hyperintensity (Fig 1A) or T2 hypointensity predominating in the peripheral and posterior parts of the lentiform nuclei, or T1 hyperintensity, T1 hypointensity, or T1 and T2 marked heterogeneity (Fig 1B and C). Basal ganglia involvement in group 2 appeared as fuzzy or tumefied areas on T1- or T2-weighted images (Fig 2B) or as T2 hyperintense (Fig 2B and C, Fig 3D) or T1 hypointense areas.

Concomitant signal changes in the posterior limb of the internal capsule were revealed by one MR imaging study (Fig 1B and C) in the two groups of children as T1 and T2 prolongation. In both groups, basal ganglia involvement tended to evolve with time from a fuzzy aspect with various signal changes to basal ganglia atrophy and T2 hyperintensity.

The injection of contrast material was performed in 20 MR imaging studies. Meningeal enhancement was observed in one MR imaging study in group 1; cortical enhancement was seen in 1 MR imaging study in group 1 and in five MR imaging studies in group 2. Basal ganglia enhancement was detected in one MR imaging study in group 2.

Cerebellar involvement, appearing as cortical tumefaction and/or T2 prolongation, was present in four MR imaging studies in group 1. It appeared as cortical patchy T2 prolongation (in six MR imaging studies) or as white matter focal T2 prolongation (in two MR imaging studies) in group 2. Data regarding interobserver agreement in the assessment of the scoring system, as determined by using the weighted kappa statistics, showed that interobserver agreement was very good ($\kappa = 0.933$; 95% confidence interval: 0.896, 0.970; $P < .001$).

Neurodevelopmental Evolution

Sixteen (40%) of the children died between days 2 and 40 after the onset of coma. Ten of the 24 surviv-

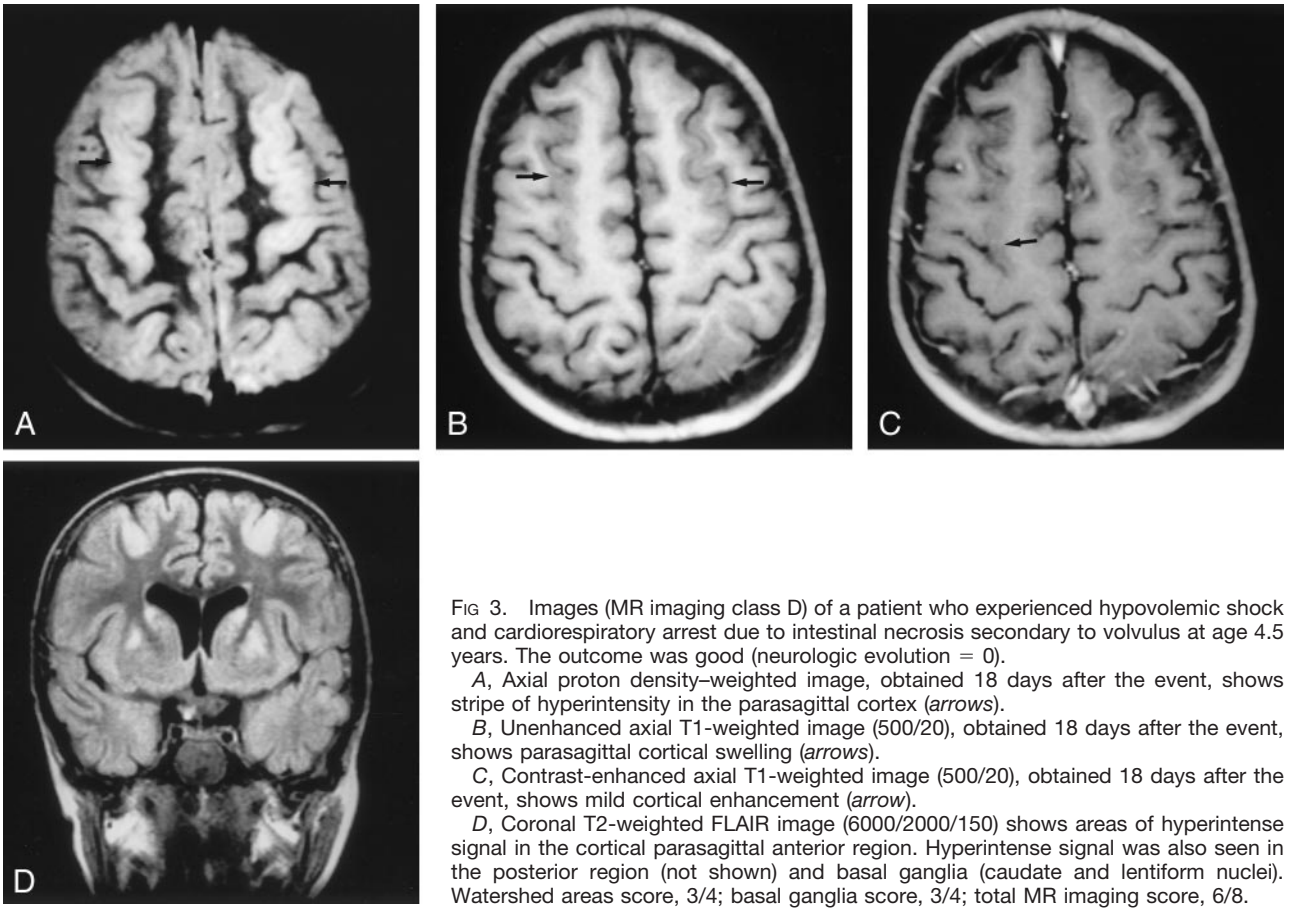

FIG 3. Images (MR imaging class D) of a patient who experienced hypovolemic shock and cardiorespiratory arrest due to intestinal necrosis secondary to volvulus at age 4.5 years. The outcome was good (neurologic evolution = 0).

A, Axial proton density–weighted image, obtained 18 days after the event, shows stripe of hyperintensity in the parasagittal cortex (*arrows*).

B, Unenhanced axial T1-weighted image (500/20), obtained 18 days after the event, shows parasagittal cortical swelling (*arrows*).

C, Contrast-enhanced axial T1-weighted image (500/20), obtained 18 days after the event, shows mild cortical enhancement (*arrow*).

D, Coronal T2-weighted FLAIR image (6000/2000/150) shows areas of hyperintense signal in the cortical parasagittal anterior region. Hyperintense signal was also seen in the posterior region (not shown) and basal ganglia (caudate and lentiform nuclei). Watershed areas score, 3/4; basal ganglia score, 3/4; total MR imaging score, 6/8.

ing children had moderate to severe mental and motor disabilities (neurologic evolution >2 and ≤8), and two experienced persistent vegetative state (neurologic evolution >8). Twelve children experienced good outcomes (neurologic evolution score ≤2), including four children without any neurologic deficits (neurologic evolution score = 0).

There were no significant differences between the two age groups ($P = .168$). No correlation was found between PRISM score and neurologic evolution ($r_s = -0.086$; $P = .598$). A strong correlation was found between first MR imaging score and neurologic evolution score ($r_s = 0.676$; $P < .001$). The impact of the MR imaging timing is summarized Table 4 in terms of sensitivity, specificity, false positive, false negative, positive predictive value, negative predictive value, and overall accuracy to predict neurologic evolution.

Normal or subnormal first MR imaging findings (score ≤2) were associated with good neurologic outcome (neurologic evolution score ≤2), with a total negative predictive value of 86% reflecting one false negative result observed in class A. Conversely, a

TABLE 3: Findings at first MR imaging and neurologic evolution

MR Imaging Findings	Good Evolution	Bad Evolution		Total
		Moderate to Severe Sequelae	Vegetative State or Death	
(Sub)normal	6	0	1	7
Abnormal	6	10	17	33
Total ($P < .001$)	12	10	18	40
Sensitivity, 27/28 (96%)				
Specificity, 6/12 (50%)				
False positive, 6/12 (50%)				
False negative, 1/28 (4%)				
Positive predictive value, 27/33 (82%)				
Negative predictive value, 6/7 (86%)				
Overall accuracy, 33/40 (82%)				

Note.—Good neurologic evolution indicates neurologic evolution score ≤2; bad neurologic evolution, neurologic evolution score >2; moderate to severe sequelae, neurologic evolution score ≥2 to <8; vegetative state or death, neurologic evolution score ≥8 to 10; abnormal MR imaging finding, MR imaging score >2; normal or subnormal MR imaging finding, MR imaging score ≤2.

TABLE 4: Impact of delay of MR imaging to predict neurologic evolution

	MR Imaging Class					
	A	B	C	D	E	Total
No. of images	10	15	14	19	6	64
Sensitivity (%)	89	100	100	100	100	98
Specificity (%)	100	75	33	20	0	35
False positive	0	1	2	4	4	11
False negative	1	0	0	0	0	1
Positive predictive value (%)	100	92	85	83	33	81
Negative predictive value (%)	50	100	100	100	0	86
Overall accuracy (%)	90	93	86	79	33	81

Note.—A indicates MR imaging on days 1–3; B, MR imaging on days 4–7; C, MR imaging on days 8–15; D, MR imaging on days 16–50; E, MR imaging after day 50.

definitely abnormal MR imaging finding (score >2) was associated with bad neurologic outcome (neurologic evolution >2), with a total positive predictive value of abnormal MR imaging findings of 81%, reflecting 11 false positive results (Table 3).

Cardiac arrest lasting >5 min was not associated with bad neurologic evolution, neither for children 1 year and younger ($\chi^2 = 0.22$; $P = 1.000$) nor for older children ($\chi^2 = 1.25$; $P = .373$). Basal ganglia damage was associated with bad neurologic evolution in children older than 1 year ($\chi^2 = 4.43$; $P = .035$) but not in children 1 year and younger. There were no significant differences in the distribution of the two main groups of hypoxia (ischemic and anoxic-hypoxic) ($P = .258$).

Discussion

This study shows a variety of MR imaging abnormalities associated with hypoxic coma in children, involving the watershed areas and the basal ganglia. The proposed MR imaging scoring system correlated with neurologic outcome.

Although the majority of children in our study experienced bad outcomes, 30% experienced good neurologic evolution. This supports a generally better prognosis of hypoxic coma in children as compared with adults (2), which may be related to greater plasticity in the developing brain. However, children 1 year and younger did not experience significantly better neurologic evolution than did older children in our study.

The children in this study constitute a heterogeneous group because of the nature of the insult. Although from a pathophysiological standpoint, cerebral hypoxia may be due to distinct mechanisms, several factors usually occur in conjunction with hypoxia (7, 13, 17, 21). This may explain the lack of correlation between neurologic evolution and cause of hypoxia.

Interpretation of MR imaging findings of children who have suffered hypoxic events may be difficult. Although focal ischemic infarcts can be clearly identified on MR images on the first day after insult in >80% of cases (13), diffuse hypoxic-ischemic lesions are more difficult to assess. Therefore, a systematic scoring system with good interobserver agreement for determining severity of brain injury may be useful.

The pattern and severity of brain lesions depend on the severity and duration of hypoxia and on the state of brain maturation at the time of injury. Severity of hypoxia may be assessed by the PRISM score, as it depends on hemodynamic and respiratory parameters and their metabolic consequences. We used the PRISM score because it is a validated, objective assessment based on a wide range of physiological variables routinely recorded in pediatric intensive care units. Its advantages over the modified Glasgow Coma Scale score include largely unbiased data collection, weighted parameters, and some categories based on age (≤1 year and >1 year), so that the PRISM score reflects the severity of illness. The Glasgow Coma Scale score has been validated in patients with traumatic coma, which is not directly relevant to our population. However, it is included as one of the 14 variables in PRISM scoring. The range of Glasgow Coma Scale scores in our study was 3 to 12. However, the median was 3, which suggests a floor effect.

The PRISM score was devised to assess the expected mortality rates for a group of children treated in a pediatric intensive care unit and not to estimate individual neurologic prognosis. Accordingly, there was no correlation between PRISM score and neurologic evolution in our study.

More than 3–5 minutes of complete brain circulation arrest is generally considered to cause definitive brain lesions (13, 16). However, in our study, cardiac arrest lasting >5 minutes was not correlated with particularly bad neurologic evolution. This might be related to difficulties in appreciating the precise duration of cardiac arrest from the patient's history. Furthermore, brain maturation influences the susceptibility of various cerebral regions to hypoxia because of maturational changes in vascular autoregulation and regional metabolic activity (7, 17).

MR imaging findings of diffuse hypoxic-ischemic lesions may be complex and subtle, varying with patient age and time of study. Knowledge of the normal aspect of brain maturation is fundamental. We did not find any significant difference in occurrence of watershed areas or basal ganglia involvement according to age groups. However, the pattern of signal changes was more varied in the group of children 1

year and younger than in the group of older children in our study.

Although MR imaging findings varied with delay of MR imaging, some features could be observed through several classes (Table 2). The MR imaging scoring system was based on two basic lesion categories, watershed areas and basal ganglia involvement, because the former is classically observed in patients with hypoxia or hypotension and the latter is commonly reported in patients with cardiocirculatory arrest (4, 10, 17). Watershed areas were located mainly in end zones in the depth of sulci and in the arterial border zones of the major cerebral arteries, mostly in the parasagittal regions. Morphologic and signal modifications were already present 12 hours after the event in the more precociously investigated child in our study.

Persistent swelling and signal changes were probably related to delayed neuronal death due to secondary neurotoxic metabolic events (16) or gliosis (8). Delayed morphologic changes consisted of global parenchymal atrophy of varying degrees, observed as ventriculomegaly and enlarged cisterns and sulci. Atrophic gyri surrounded by wide sulci may have the characteristic mushroom pattern of ulegyria. It is noteworthy that atrophy may be difficult to differentiate from pseudoatrophy related to the nutritional status of children treated in an intensive care unit.

There were some differences between the MR imaging findings related to age. In children 1 year and younger, edema and necrosis involve not only the cortex but also the white matter, as observed in neonates with hypoxic-ischemic encephalopathy (3–10). This may be due to increased vulnerability associated with active myelination. This process requires high energy consumption, leading to increased susceptibility to hypoxic-ischemic injury (17).

Morphologic signs were best seen on T1-weighted images and were probably related to cytotoxic edema. Signal intensity modifications were best observed on T2- or proton density–weighted images and were likely due to vasogenic edema and/or cellular necrosis. Cortical hyperintensities on T1-weighted images may be related to increased concentration of denatured proteins released by cell necrosis or blood-brain barrier breakdown (6, 14), fat-laden macrophages (15, 16), calcifications, or petechial hemorrhages (16) (methemoglobin) in reperfused ischemic areas. Localized cortical T2 hypointensities may be due to paramagnetic effect of free radicals, hemorrhage (deoxyhemoglobin, hemosiderin), or neuronal mineralization (8).

In children older than 1 year, white matter is commonly considered to be less vulnerable to hypoxia than is gray matter, consistent with our findings, although hypoxia may cause secondary white matter degeneration due to myelin destruction and axonal degeneration (13, 16). In our study, cortical swelling, attributed to cytotoxic and eventually vasogenic edema, was best seen on T1-weighted images. Signal changes were best appreciated on T2-FLAIR images and, to a lesser extent, on proton density- or T2-weighted spin-echo images. Coronal FLAIR sequences are particularly interesting in that they allow a comparison within the same image of the signal intensity of the supratentorial parenchyma with that of the cerebellum, the involvement of which is less often diffuse. T2 prolongation of the cortex and stripe of hyperintensity in the cortex and the subcortical white matter on T2- and proton density-weighted sequences are likely due to vasogenic edema or cell necrosis (13).

Basal ganglia involvement is related to the high metabolic activity of the basal ganglia resulting in increased sensitivity to profound hypoxia, as observed in cases of cardiac arrest (4, 17). Basal ganglia involvement may represent edema, neuronal death, gliosis, mineralization of dead neurons, abnormal capillary proliferation, or hemorrhagic necrosis (7, 8). Basal ganglia damage is usually associated with severe neurologic evolution (3, 9), as particularly evident in our group of children older than 1 year but not in younger children. The reason for this discrepancy is not obvious, as the basal ganglia are known to be more active metabolically during the first months of life (10). Moreover, we did not find a significant difference in occurrence of basal ganglia involvement between younger and older patients. In children 1 year and younger, involvement of the basal ganglia appeared mostly as hyperintense abnormal areas on T2-weighted images. Fuzzy margins, T2 prolongation, or T1 prolongation were probably due to edema and necrosis. T1 and T2 shortening predominating in the posterior part of the lentiform nuclei was present in some cases. This may be explained by the paramagnetic effect of free radicals, the presence of denatured proteins (15), hemorrhage, membrane lipids, and clusters of mineralized neurons (8, 18). High T1 and T2 heterogenicity was present in four MR imaging studies, probably owing to necrotic-hemorrhagic components. In children older than 1 year, basal ganglia involvement appeared essentially as abnormal hyperintense areas on T2-weighted images or as having fuzzy margins probably related to edema or necrosis.

The sensitivity of MR imaging was high in all classes. When analyzed by class, the best correlation with neurologic evolution was observed for class A and B MR imaging scores (overall accuracy rates of 90% and 93%, respectively) indicating that MR imaging studies performed within the first week were the most useful. This may be partially explained by the selection of patients, as relatively more severe cases (including those ending in death) were principally investigated by class A and B MR imaging. Most class A MR imaging studies could provide morphologic and signal information, primarily regarding watershed areas but also regarding basal ganglia involvement.

These results are consistent with those reported by Dubowitz et al (18), which showed good correlation between MR imaging findings and neurologic outcomes as early as the first 2 days after the event. However, these authors found that MR imaging had a better predictive value when performed beyond the third day. Other authors (4) reported a generally better predictive value of MR imaging performed

after the first week as compared with MR imaging performed during the first week. Repeat MR imaging studies might therefore aim at better detecting changes when brain damage processes are more advanced and obvious. However, repeat MR imaging was of special value in only one child in our study, the child with the single false negative result (Fig 1) whose first MR imaging study was class A, performed 28 hours after the event. Conversely, the specificity of MR imaging in our study decreased with delay. In classes B through E, 11 MR imaging studies of six children with definite abnormal MR imaging findings were associated with good neurologic evolution (Fig 3).

All the sequences that were used in the present study seemed to be complementary and should be applied to best characterize hypoxic-ischemic lesions. FLAIR imaging is widely recognized to have high sensitivity in detecting infarction in the mature brain. The role of FLAIR imaging in neonates and young children is yet to be determined, taking into account the progression of myelination (22). As with FLAIR imaging in adults, proton density-weighted imaging has a high sensitivity for detecting early hypoxic lesions in young children (4, 5). Contrast-enhanced MR imaging may be useful as soon as 3 days after insult to precisely detect the extent of brain damage (12, 13). Contrast-enhanced T1-weighted images, obtained in 20 of our MR imaging studies, indicated more severe brain damage than did unenhanced images and had a prognostic significance in the MR imaging scoring system in only one case (MR imaging performed on day 5).

A limitation of our study is the relatively small number of patients, resulting in low power statistical tests. The predictive value of MR imaging, therefore, needs to be confirmed in a larger patient sample. The developmental assessments of three children who were 1 year and younger should be considered with caution because of the short follow-up duration (1, 2, and 2.5 months). The neurologic evolution of the other 37 patients was graded 1–8 years after the hypoxic event. Furthermore, neurologic outcome issues are complex. Although vegetative state and death are generally accepted as bad outcomes, other stages of neurologic evolution can be disputed regarding classification between good and bad outcomes. Additionally, we did not compare our scoring system to nonsystematic observation.

Conclusion

The MR imaging scoring system proposed in this study can be used to establish an early prognosis in a significant proportion of children with hypoxic coma. It is helpful even during the first 3 days after the event. However, some patients with definite abnormal MR imaging findings may experience good neurologic evolution. This study suggests that conventional MR imaging techniques may be helpful for clinical decisions and may be of great interest for the evaluation of new modalities of therapy to prevent secondary cell death.

References

1. Zandbergen EJ, de Haan RJ, Stoutenbeek CP, Koelman JH, Hijdra A. **Systematic review of early prediction of poor outcome in anoxic-ischaemic coma.** *Lancet* 1998;352:1808–1812
2. Chen R, Bolton CF, Young GB. **Prediction of outcome in patients with anoxic coma: a clinical and electrophysiologic study.** *Crit Care Med* 1996;24:672–678
3. Rutherford M, Pennock J, Schwieso J, Cowan F, Dubowitz L. **Hypoxic-ischaemic encephalopathy: early and late magnetic resonance imaging findings in relation to outcome.** *Arch Dis Child Fetal Neonatal Ed* 1996;75:F145–F151
4. Barkovich AJ, Hajnal BL, Vigneron D, et al. **Prediction of neuromotor outcome in perinatal asphyxia: evaluation of MR scoring systems.** *AJNR Am J Neuroradiol* 1998;19:143–149
5. Christophe C, Clercx A, Blum D, Hasaerts D, Segebarth C, Perlmutter N. **Early MR detection of cortical and subcortical hypoxic-ischemic encephalopathy in full-term-infants.** *Pediatr Radiol* 1994;24:581–584
6. Rutherford MA, Pennock JM, Schwieso JE, Cowan FM, Dubowitz LM. **Hypoxic ischaemic encephalopathy: early magnetic resonance imaging findings and their evolution.** *Neuropediatrics* 1995;26:183–191
7. Volpe JJ. **Value of MR in definition of the neuropathology of cerebral palsy in vivo.** *AJNR Am J Neuroradiol* 1992;13:79–83
8. Felderhoff-Mueser U, Rutheford MA, Squier WV, et al. **Relationship between MR imaging and histopathologic findings of the brain in extremely sick preterm infants.** *AJNR Am J Neuroradiol* 1999;20:1349–1357
9. Mercuri E, Guzzetta A, Haataja L, et al. **Neonatal neurological examination in infants with hypoxic ischaemic encephalopathy: correlation with MRI findings.** *Neuropediatrics* 1999;30:83–89
10. Barkovich AJ, Westmark K, Patridge C, Sola A, Ferriero DM. **Perinatal asphyxia: MR findings in the first 10 days.** *AJNR Am J Neuroradiol* 1995;16:427–438
11. Mercuri E, Rutherford M, Cowan F, et al. **Early prognostic indicators of outcome in infants with neonatal cerebral infarction: a clinical, electrocephalogram, and magnetic resonance imaging study.** *Pediatrics* 1999;103:39–46
12. Westmark KD, Barkovich AJ, Sola A, Ferriero D, Partridge JC. **Patterns and implications of MR contrast enhancement in perinatal asphyxia: a preliminary report.** *AJNR Am J Neuroradiol* 1995;16:685–692
13. Beauchamp NJ, Barker PB, Wang PY, van Zijl PC. **Imaging of acute cerebral ischemia.** *Radiology* 1999;212:307–324
14. Komiyama M, Nakajima H, Nishikawa M, Yasui T. **Serial MR observation of cortical laminar necrosis caused by brain infarction.** *Neuroradiology* 1998;40:771–777
15. Komiyama M, Nakajima H, Nishikawa M, Yasui T. **Chronological changes in nonhaemorrhagic brain infarcts with short T1 in the cerebellum and basal ganglia.** *Neuroradiology* 2000;42:492–498
16. Takahash S, Higano S, Ishii K, Matsumoto K, et al. **Hypoxic brain damage: cortical laminar necrosis and delayed changes in white matter at sequential MR imaging.** *Radiology* 1993;189:449–456
17. Barkovich AJ. **MR and CT evaluation of profound neonatal and infantile asphyxia.** *AJNR Am J Neuroradiol* 1992;13:959–975
18. Dubowitz DJ, Bluml S, Arcinue E, Dietrich RB. **MR of hypoxic encephalopathy in children after near drowning: correlation with quantitative proton MR spectroscopy and clinical outcome.** *AJNR Am J Neuroradiol* 1998;19:1617–1627
19. Pollack MM, Ruttimann UE, Getson PR. **Pediatric risk of mortality (PRISM) score.** *Crit Care Med* 1988;16:1110–1116
20. StatXact 3 for windows. *Statistical Software for Exact Nonparametric Inference: User Manual.* Cambridge: CYTEL Software Corporation; 1995
21. Marret S, Zupan V, Gressens P, Lagercrantz H, Evrard P. **Periventricular leukomalacia and brain protection: II. diagnosis, sequelae and neuroprotection [in French].** *Arch Pediatr* 1998;5:538–545
22. Murakami JW, Weinberger E, Shaw DW. **Normal myelination of the pediatric brain imaged with fluid-attenuated inversion-recovery (FLAIR) MR imaging.** *AJNR Am J Neuroradiol* 1999;20:1406–1411